Carbon Letters
https://doi.org/10.1007/s42823-019-00084-2

Online ISSN 2233-4998
Print ISSN 1976-4251

ORIGINAL ARTICLE

Carbonaceous catalysts from orange pulp for limonene oxidation

Agnieszka Wróblewska[1] · Jarosław Serafin[2] · Alicja Gawarecka[1] · Piotr Miądlicki[1] · Karolina Urbaś[3] · Zvi C. Koren[4] · Jordi Llorca[5] · Beata Michalkiewicz[2]

Received: 18 March 2019 / Revised: 25 July 2019 / Accepted: 9 August 2019

Abstract
The possibility of orange pulp utilization for nanoporous carbons production was investigated. Moreover, processing the obtained materials as limonene oxidation catalysts was studied as well. Limonene was separated from orange pulp obtained from fragmented orange peels—the waste from industrial fruits processing—by means of simple distillation. After the separation of limonene from the biomass, the dried orange pulp was converted to three types of nanoporous carbon catalysts: without activating agent, with NaOH, and with KOH. The catalysts were characterized by XRD, SEM, EDX, AFM, and sorption of N_2 methods. The activities of the obtained catalysts were tested in the oxidation of limonene to perillyl alcohol (the main product), carveol, carvone, and 1,2-epoxylimonene and its diol. In the oxidation processes, hydrogen peroxide was used as the oxidizing agent. This work has shown for the first time that nanoporous carbons obtained from orange pulp waste, after separation of limonene, are active catalysts for limonene oxidation to industrially important value-added products.

Keywords Orange pulp · Nanoporous carbon catalysts · Limonene oxidation · Perillyl alcohol

1 Introduction

The orange juice industry is a source of 8–20 million tons of waste material globally [1]—mainly in the form of fragmented orange peels and the membranes from inside the fruit. These remains represent an environmental problem due to microbial spoilage [2, 3]. However, this biomass can be a valuable source of natural limonene, the main component of the orange essential oil [4, 5], and it can be separated from the pulp by simple distillation. The purity of the obtained natural limonene can reach 98%. In this form, it can be used as a raw material in organic syntheses, for example, with an additional ecologically friendly compound—hydrogen peroxide as an oxidant.

Limonene has antibacterial, antifungal, and insecticidal activity [6]. Among the derivatives of limonene, especially important are its oxygenated derivatives (perillyl alcohol, carveol, carvone, 1,2-epoxylimonene, and 1,2-epoxylimonene diol), which are far more industrially valuable

Electronic supplementary material The online version of this article (https://doi.org/10.1007/s42823-019-00084-2) contains supplementary material, which is available to authorized users.

✉ Beata Michalkiewicz
beata.michalkiewicz@zut.edu.pl

[1] Faculty of Chemical Technology and Engineering, Institute of Organic Chemical Technology, West Pomeranian University of Technology, Szczecin, Pulaskiego 10, 70-322 Szczecin, Poland

[2] Faculty of Chemical Technology and Engineering, Institute of Inorganic Chemical Technology and Environment Engineering, West Pomeranian University of Technology, Szczecin, Pulaskiego 10, 70-322 Szczecin, Poland

[3] Faculty of Chemical Technology and Engineering, Department of Nanomaterials and Physicochemistry, West Pomeranian University of Technology, Szczecin, Al. Piastów 49, 71-899 Szczecin, Poland

[4] Department of Chemical Engineering, Shenkar College of Engineering, Design and Art, 12 Anna Frank St, 52526 Ramat Gan, Israel

[5] Institute of Energy Technologies, Department of Chemical Engineering, Barcelona Research Center in Multiscale Science and Engineering, Universitat Politècnica de Catalunya, EEBE, Eduard Maristany 16, 08019 Barcelona, Spain

Published online: 23 August 2019

compounds than limonene itself. Moreover, we can obtain such compounds with very high selectivity depending on the process conditions and the catalyst that is used. These compounds have many applications as components of fragrant compositions for perfumery and cosmetics, as food additives, and as components of polymers. In medicinal applications, perillyl alcohol has been shown to be efficacious against the formation and progression of cancers of the colon, skin, head, lung, and neck [7, 8]. Carveol, the second oxygenated derivative of limonene, is also used as an anticancer agent for the therapy of pancreatic and breast cancers [9, 10], and also shows anti-yeast and antifungal activity.

Commonly, carbonaceous materials are applied in water purification [11], gas separation, sensors, sequestration, and energy storage [12, 13]. Carbonaceous materials have also been described as supports for catalysts. Activated carbon-supported metal catalysts have been applied in nitric oxide reduction [14], gasification of biomass hydrolysates by aqueous-phase reforming [15], oxidation of glycerol to lactic acid [16], ethanol oxidation [17], and alkene oxidation [18]. Carbonaceous materials without any additives were seldom described as catalysts. To make them active in biodiesel production, carbonaceous materials had to be functionalized by sulfuric acid and oleum [19, 20].

Activated carbons as catalysts for limonene oxidation were described only by our team [21, 22]. The method of nanoporous carbon production from orange pulp after limonene extraction was not described up to now, and some of the authors of this manuscript are inventors of the Polish-pending patent [23]. Our work shows the possibility of utilizing the orange peels waste from industrial fruits processing, both as a source of important oxygenated limonene derivatives, and also, after separation of limonene, as a source of nanoporous carbon catalysts for the oxidation of limonene to these products.

2 Materials and methods

2.1 Materials

For the synthesis of the catalysts, tetraethyl orthosilicate (TEOS) obtained from Sigma-Aldrich was used. Aqueous ammonia solution (25–28 wt %) and ethanol (96% purity) were acquired from Chempur, Poland. Analytical grade NaOH and KOH were supplied from Eurochem BGD. Limonene was obtained by distillation from orange pulp (98% purity). In the limonene oxidation, the following reagents were also used: methanol (analytical grade) and 60 wt % aqueous solution of hydrogen peroxide (both from Chempur).

2.2 Preparation of catalysts from dried orange pulp residue (after limonene distillation)

First, silica nanosphere templates were prepared by suitably modifying a previously reported procedure [24, 31], as follows. Deionized water, NH_3(aq), and C_2H_5OH were successively added to TEOS in the volume ratios of 3:1:23:2, respectively. The resulting mixture was then stirred for 3 h at room temperature. The white colloidal suspension that was obtained was centrifuged and washed three times with deionized water, followed by an ethanol washing. Subsequently, silica nanosphere particles were obtained.

Nanoporous carbon was obtained by mixing dried orange pulp (after limonene extraction) with the silica nanospheres in the mass ratio of 10:1, respectively. Water was added dropwise onto the residue until incipient wetness was observed. This method is a well-established technique for catalyst production [25], which was described in detail in other works [26, 27]. The mixture was dried at a temperature of 80 °C during 2 h followed by a temperature of 160 °C for 16 h. The pyrolysis was performed in a tubular furnace at 750 °C for 2 h. To remove the silica templates, the product of the pyrolysis was stirred in an aqueous HF solution (7 wt %) for 24 h, followed by filtration, washing with deionized water, and drying at 200 °C for 12 h. Finally, nanoporous carbon, denoted as OR, was obtained.

To obtain more porous carbon materials, KOH and NaOH were added before carbonization. The mass ratio of dried orange pulp, silica nanospheres, and hydroxide was equal to 10:1:10, respectively.

2.3 X-ray diffraction

The XRD scans were performed on a PANalytical X-ray Empyrean diffractometer using Cu Kα radiation. The samples were prepared by packing finely ground powders into holders covered by a glass slide to produce a dense agglomerate of powder with a flat surface necessary for XRD studies. The spectra were analyzed using X'Pert HighStore diffraction software.

2.4 Nitrogen sorption

Prior to N_2 sorption measurements, the samples were degassed overnight at 250 °C. The surface area (S_{BET}), total pore volume (V_{tot}), and micropore volume (V_{micro}) of the samples were determined by nitrogen adsorption at 77 K. The measurements were performed via the Surface Area & Pore Size Analyzer Quadrasorb evo provided by Quantachrome Instruments. Data were collected from a relative pressure (p/p_0) range of 0.002–0.99. The specific surface

area was calculated using the Brunauer–Emmett–Teller (BET) adsorption isotherm model [28] from the slope and *y*-intercept of the linear region of the $1/[W(p_0/p-1)]$ versus p/p_0 plot, where W is the weight of gas adsorbed at a relative pressure, p/p_0 [29]. The total pore volume was calculated according to the Gurvitch method for $p/p_0 = 0.99$ [37]. Density functional theory (DFT) model predictions of pore size distributions were calculated using the DFT Library [30, 31]. The model assumed a mixed slit/cylindrical pore geometry. The total pore volume was estimated from N_2 adsorption data as volume of liquid N_2 at p/p_0 equal to 0.99 [32]. The micropore volume (V_{mic}) was estimated by the DTF method [15, 33, 34].

2.5 SEM, EDX, and AFM analyses

Scanning electron microscopy images were obtained using ultrahigh-resolution field-emission scanning electron microscope (UHR FE–SEM Hitachi SU8020). Energy-dispersive X-rays (EDX) spectra were collected and analyzed on NSS 3.0 software. Samples for SEM/EDX analysis were attached on an aluminum sample holder using a double-stick electrically conductive carbon tape. The surface morphology of the samples was also studied by atomic force microscopy (AFM) with a Bruker NanoScope V SPM (Scanning Probe Microscope) working in MultiMode.

2.6 Method of limonene oxidation

The epoxidations of limonene were performed for the reaction time of 6 h at the following temperatures (°C): 80, 100, 120, and 140. The other parameters were as follows: the molar ratio of limonene/H_2O_2 = 1:2, methanol concentration 70 wt %, and the catalyst content in the reaction mixture was 4 wt %. The process was performed in an autoclave with the TEFLON insert with a capacity of 100 cm^3 and equipped with a magnetic stirrer. The raw materials were placed into the autoclave in the following order: catalyst, limonene, methanol, and 60 wt % aqueous solution of hydrogen peroxide.

Samples were analyzed by a GC method on a Focus apparatus equipped with a flame-ionization detector and fitted with the Restek Rtx-WAX capillary column filled with polyethylene glycol. The parameters of the GC method were as follows: helium pressure of 50 kPa, sensitivity of 100, temperature of the sample chamber 200 °C, and detector temperature of 250 °C. The temperature of the thermostat was increased according to the following program: isothermally at 60 °C for 2 min, an increase to 240 °C at the rate of 15 °C/min, isothermally at 240 °C for 4 min, and at the last stage, cooling to 60 °C. The products of limonene oxidation were also qualitatively identified by the GC–MS method.

3 Results and discussion

3.1 Catalyst characterization

Table 1 shows the semiquantitative compositions of the elements in the produced materials as measured by the EDX method. Based on the results, we concluded that the orange pulp contains considerable amounts of Ca. The presence of fluorine is essentially due to the HF that was used for silica removal.

The specific crystalline phases present in the samples were indicated by labelling the major peaks in Fig. 1. Results of the XRD measurements indicated that fluorine could not be completely removed by washing because of the reaction with the other elements: Ca, K, and Na. The OR nanoporous carbon had significant graphite peaks of (0 0 2) and (1 0 0) at about 26° and 45°, but the peaks were very broad because of the random turbostratic stacking of layers. Five broad peaks at 28, 47, 56, 69, and 76° theta corresponded to (1 1 1), (2 2 0), (3 1 1), (4 0 0), and (3 3 1) planes, respectively, and can be identified as cubic calcium fluoride (JCPDS: 77-2096) or cubic silicon (JCPDS: 05-0565). On the basis of the EDX measurements, the presence of both can be assumed. These peaks still existed in the ORKOH and ORNaOH materials.

The appearance of sharp peaks in the ORNaOH sample (Fig. 1b) is attributed to the formation of a hexagonal crystalline sodium hexafluorosilicate, Na_2SiF_6, phase (JCPDS: 33-1280). The broad graphite peaks can be seen as well.

For the ORKOH-activated carbon (Fig. 1c), the major phase that was observed was potassium hexafluorosilicate, K_2SiF_6 (JCPDS: 75-0694). The carbon structures appear to be absent, because graphite peaks are not visible in the ORKOH spectrum and can also be due to the very intense and sharp peaks of the main phase. The EDX results confirmed the presence of carbon.

The isotherm (Supplementary Fig. 1) measured for the OR catalyst exhibited a sharp increase in the adsorbed

Table 1 Results of EDX measurements for the nanoporous carbon materials

Element	OR (wt %)	ORNaOH (wt %)	ORKOH (wt %)
C	55.8	7.9	32.1
O	5.1	5.3	6.4
F	12.4	57.1	38.0
Na	0.2	17.9	0.1
Mg	0.8	0.3	0.2
Si	1.0	0.9	1.1
K	1.1	1.0	11.0
Ca	23.6	9.6	11.1

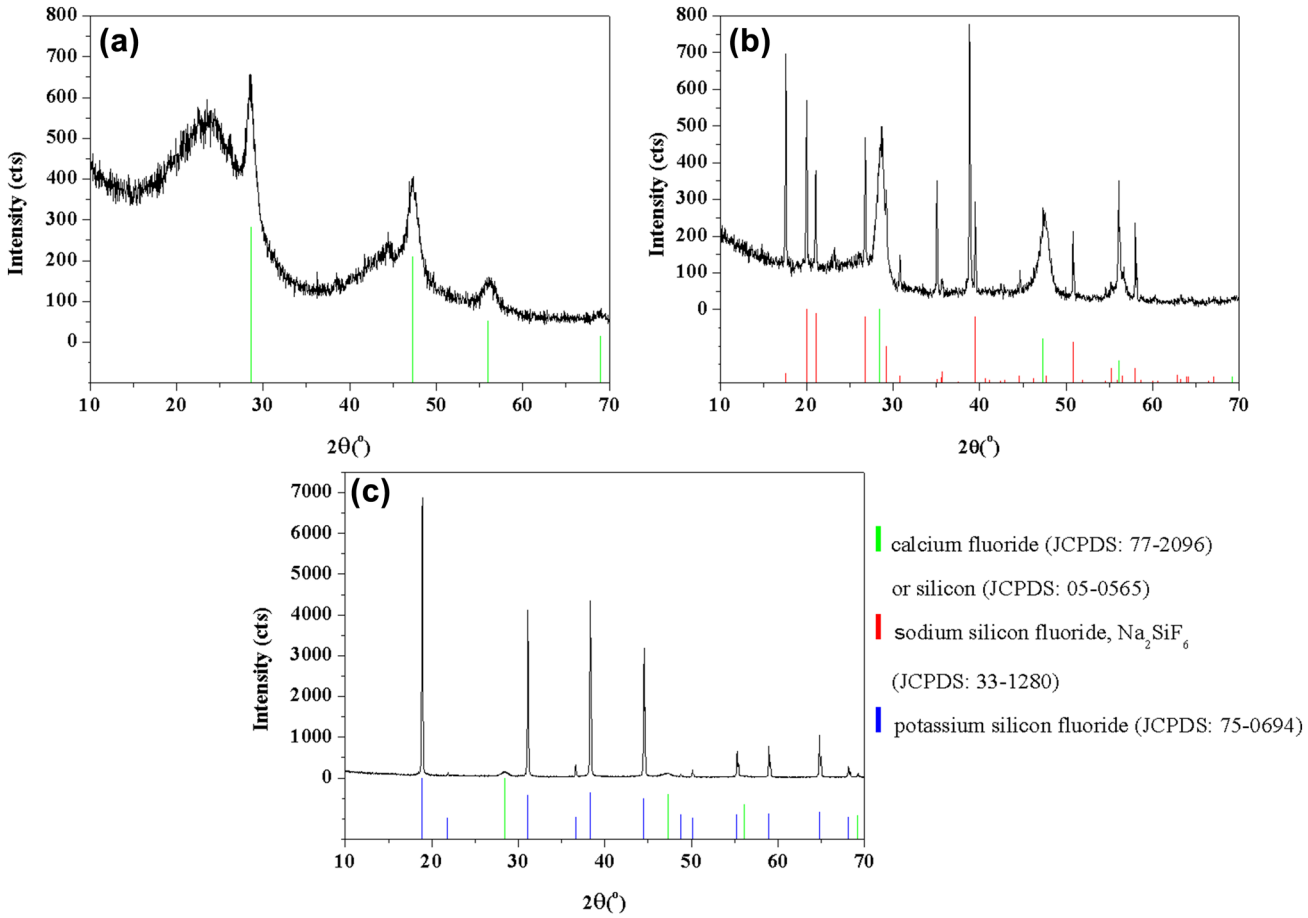

Fig. 1 XRD diffractions of (**a**) OR, (**b**) ORNaOH, and (**c**) ORKOH

nitrogen volume at very small p/p_0 values, which is characteristic of microporous materials. The presence of hysteresis in the p/p_0 plot suggests that there are mesopores in the OR catalyst [35]. The OR had isotherms of type IV with H2 mixed with H4 hysteresis loops. Such hysteresis, showing a delayed desorption, is typical for mesoporous materials with constricted pores [36]. The hysteresis loop was not closed, which suggested an insufficient connectivity of the pore network that inhibits desorption [37]. The corresponding pore size distribution (PSD) confirms the presence of micropores and small mesopores up to 10 nm (Supplementary Fig. 2).

The ORNaOH and ORKOH catalysts had isotherms (Supplementary Fig. 1) of type V with H3 hysteresis loop, which does not exhibit any limiting adsorption at high p/p_0. The H3 hysteresis loop is observed with aggregates of plate-like particles giving rise to slit-shaped pores. Micropores were absent in ORNaOH and ORKOH, and their mesopore volume was considerably lower than in OR. Table 2 summarizes the textural properties of the samples. The small amounts of micropores and mesopores were due to the very low presence of nanoporous carbon in the samples.

Table 2 Textural properties of the samples

Sample	S_{BET} (m^2/g)	V_{tot} (cm^3/g)	V_{micro} (cm^3/g)
OR	422	0.262	0.131
ORKOH	47	0.096	0.007
ORNaOH	32	0.161	0.003

The SEM and AFM images show the textures of the samples (Figs. 2, 3, 4). The OR material showed well-structured order with a hollow center of a nanoporous carbon material. The diameters of the pores were similar to the diameters of the silica nanospheres (about 310 nm). This suggests that the structure of the template was well replicated. The pores were developed during thermal treatment followed by template removal. The depth of the cavities was about 150 nm. Introduction of NaOH and KOH affected the morphology of the carbonaceous catalysts. Upon the incorporation of NaOH and KOH into the mixture of orange pulp and silica nanospheres, the template was damaged and the morphology of ORNaOH and ORKOH was completely different from OR.

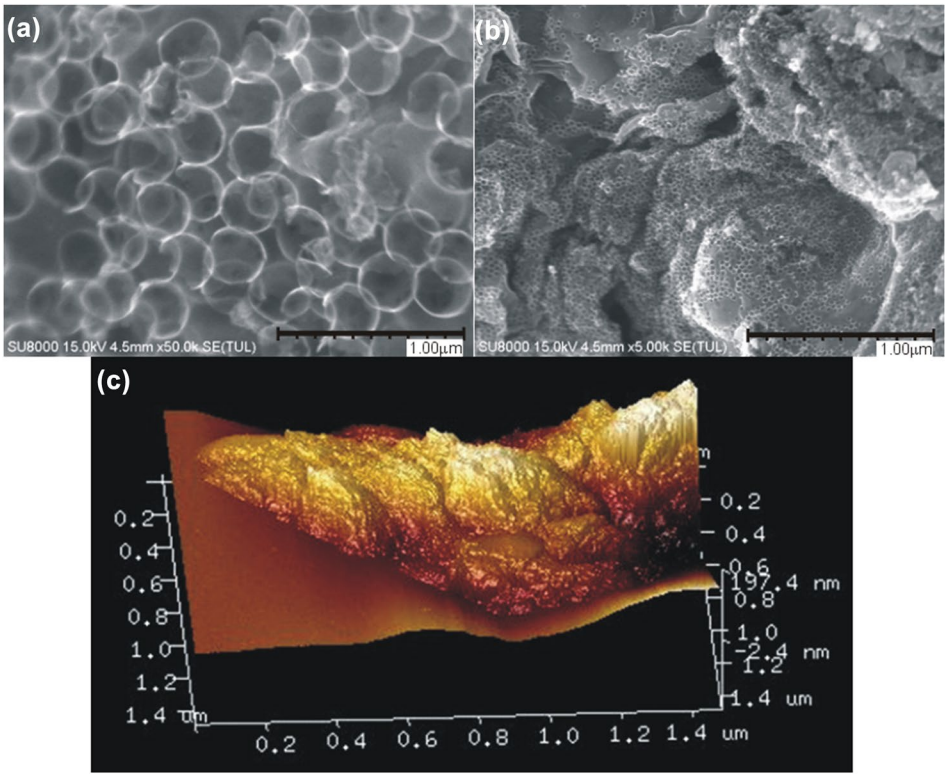

Fig. 2 Images of OR from SEM (**a** and **b**) and AFM (**c**)

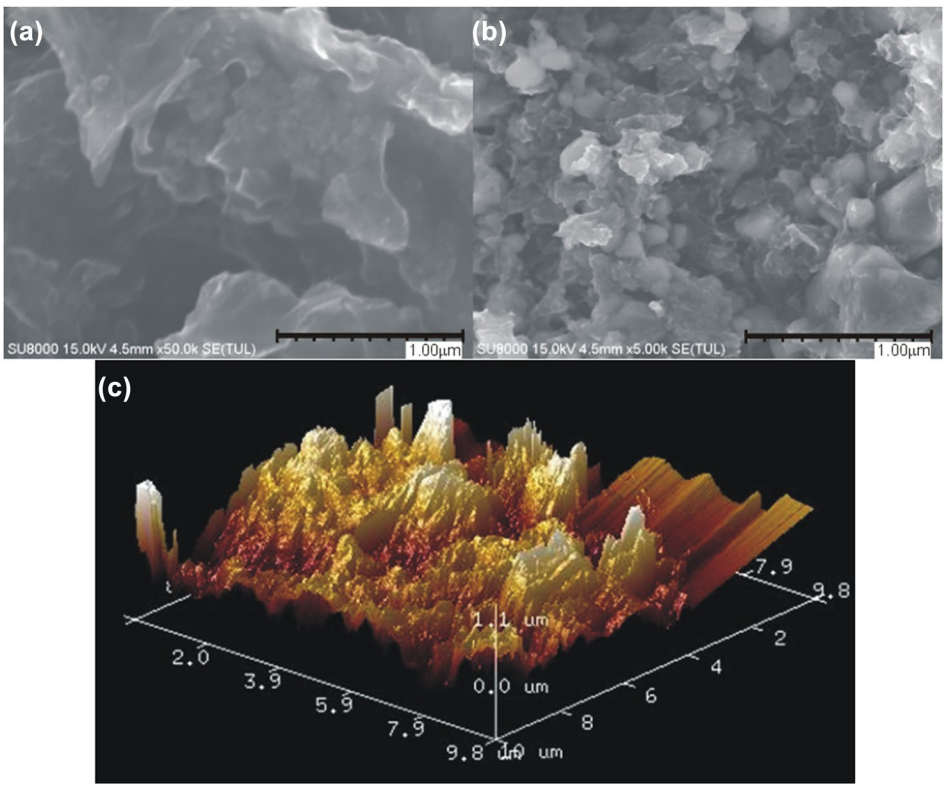

Fig. 3 Images of ORKOH from SEM (**a** and **b**) and AFM (**c**)

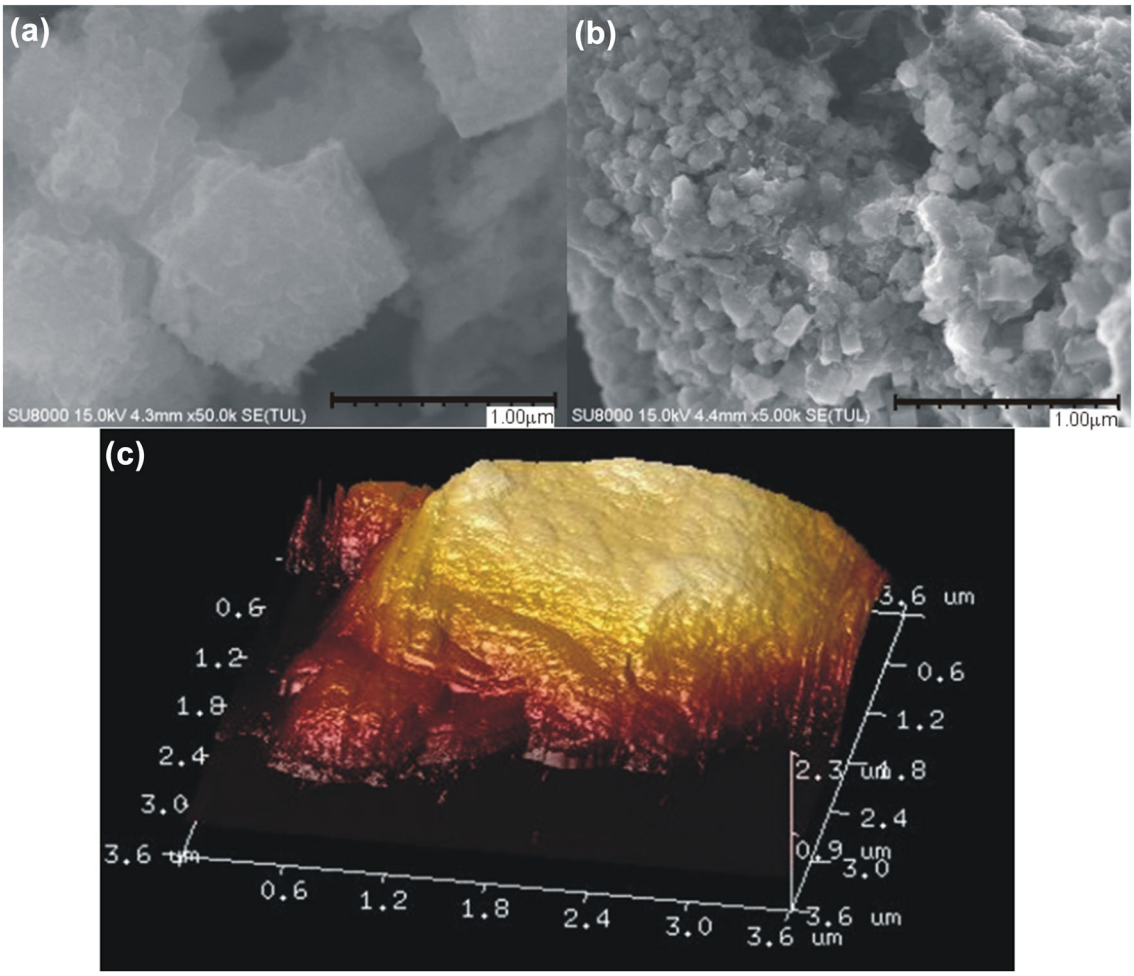

Fig. 4 Images of ORNaOH from SEM (**a** and **b**) and AFM (**c**)

The results of SEM and AFM measurements were consistent and complemented each other.

3.2 Oxidation of limonene with H_2O_2

Perillyl alcohol (the main product), carveol, carvone, and 1,2-epoxylimonene and its diol were obtained during the limonene oxidation process (Fig. 5).

The results of the studies on limonene oxidation over three catalysts obtained from orange pulp with 60 wt % water solution of hydrogen peroxide as the oxidizing agent are presented in Fig. 6a–d.

Figure 6a shows that all tested materials (OR, ORNaOH, and ORKOH) were active catalysts in the oxidation of limonene. Increasing the temperature of the oxidation from 80 to 140 °C also increases the conversion of limonene (excluding the ORNaOH catalyst at 140 °C). The most considerable increase was observed for the OR catalyst, for which the conversion of limonene increased from 4 to 42 mol %. For ORNaOH the conversion of limonene increased from 11 to 34 mol % and then decreased slightly to 29 mol %. For the ORKOH catalyst, the increase in the limonene conversion was observed from 10 to 31 mol %.

As shown in our previous work [30–32, 38, 39], the following products can be obtained as a result of the oxidation of limonene: perillyl alcohol, carveol, carvone, 1,2-epoxylimonene, and 1,2-epoxylimonene diol. The studies presented in this current work show that all these products were present in the post-reaction mixtures and the main product of limonene oxidation was perillyl alcohol, the product of the allylic oxidation at position seven in the limonene molecule.

Figure 6b shows that over the catalyst obtained without any activating agent (OR), the main direction of oxidation was the allylic oxidation at position seven in the limonene molecule. The selectivity obtained in this path caused the amount of perillyl alcohol to change slightly from 46.5 to 53.2 mol %. In addition, other directions of limonene oxidation were preferred: epoxidation at the 1,2-position to 1,2-epoxylimonene and the subsequent hydration of this

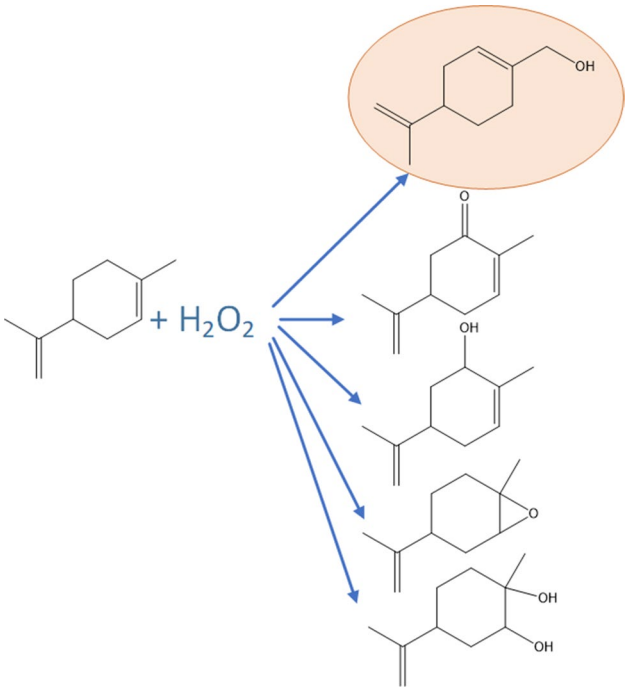

Fig. 5 Scheme of the transformation of limonene into all the products observed

compound to 1,2-epoxylimonene diol, allylic oxidation at position six and formation of carveol, and oxidation at position six and formation of carvone. From these last three oxidation directions, the preferred route was epoxidation at the 1,2-position and the formation of diol in the next step, because the combined selectivities of these two compounds was higher than the selectivity of carveol or carvone. It is also observed that the selectivity of carveol formation decreases from 17.1 to 6.8 mol %, as the temperature increases from 80 to 140 °C.

Figure 6c presents the changes of the selectivities of the products of limonene oxidation over the ORNaOH material. The results from Fig. 6c show that the preparation of the catalyst with the activator in the form of NaOH did not change the main directions of the oxidation of limonene. The main product is still perillyl alcohol, and its selectivity is comparable to that obtained over the OR catalyst and amounted to 44.5–53.6 mol %. On the other hand, there is a considerable increase in the epoxidation of the 1,2-position in the limonene molecule in comparison with the oxidation at position six (carveol and carvone formation). The selectivity of 1,2-epoxylimonene increased from 6.4 to 31.3 and 27.0 mol % and next decreased to 17.4 mol %. The selectivity of 1,2-epoxylimonene diol decreased from

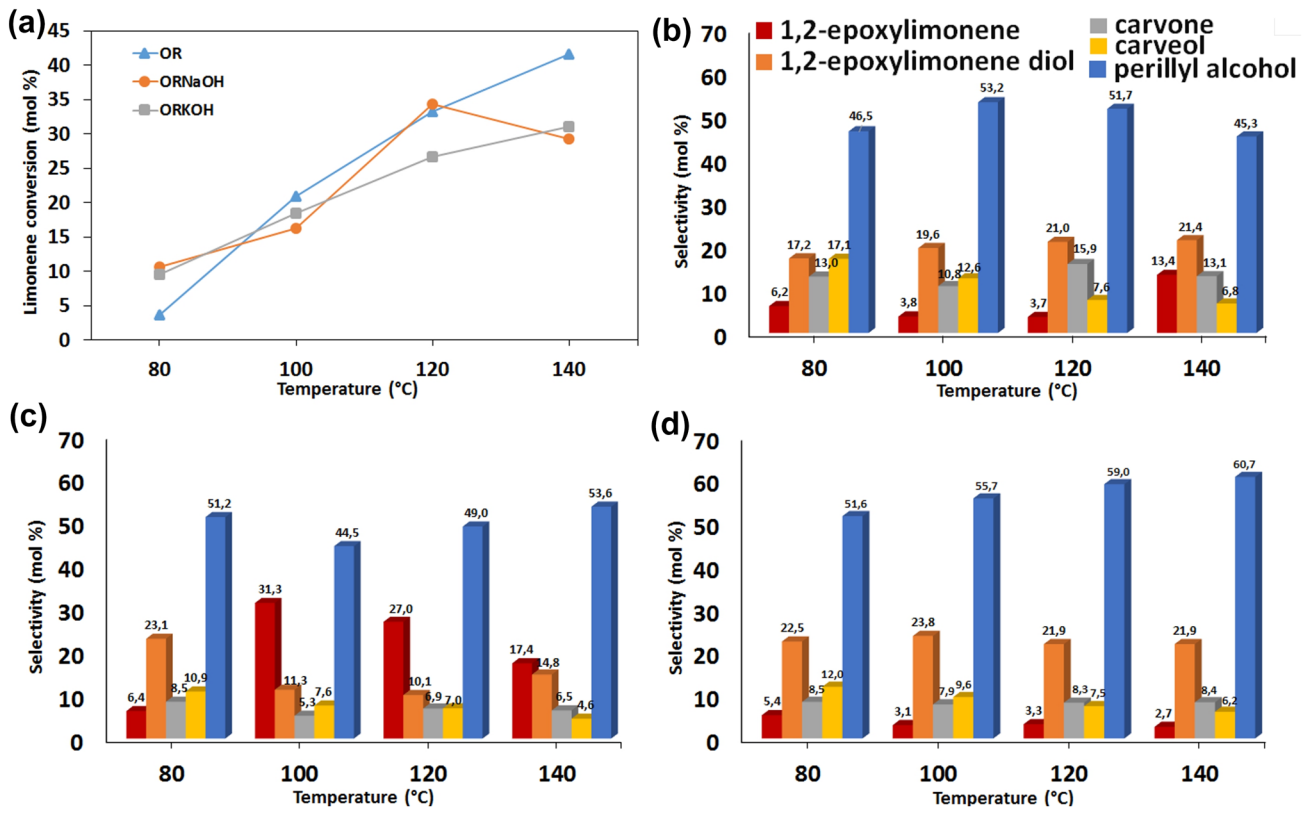

Fig. 6 Changes of limonene conversion during oxidation of limonene over OR, ORNaOH, and ORKOH catalysts in the presence of 60 wt % water solution of hydrogen peroxide as the oxidizing agent (temperatures 80–140 °C, the molar ratio limonene/hydrogen peroxide = 1:2, methanol (solvent) concentration 70 wt %, catalyst content 4 wt %, and reaction time 6 h)

23.1 to about 10–14 mol %. The selectivity of carvone was practically unchanged and amounted to about 5–8 mol %, as was the selectivity of carveol with a slight change from about 7–11 mol %.

Figure 6d presents the changes of the selectivities of the products of limonene oxidation over the ORKOH catalyst. There is an increase of 10% in the selectivity of perillyl alcohol in comparison with OR and ORNaOH catalysts. This selectivity changes from 51.6 to 60.7 mol %. This increase is mainly connected with the decrease of selectivity of 1,2-epoxylimonene, which changed from 5.4 to 2.7 mol %. There is also a noticeable increase in the selectivity of 1,2-epoxylimonene diol. It shows that 1,2-epoxylimonene was not as stable, as it was for the ORNAOH catalyst, where its selectivity was high and reached 31.3 mol %. Over the ORKOH catalyst, the epoxide compound very easily underwent hydration to diol. The selectivity of diol changed from 22.5 to 21.9 mol %. The selectivities of carveol and carvone were comparable with the selectivities of these two compounds obtained over the ORNaOH catalyst.

A comparison of the results obtained for OR, ORNaOH, and ORKOH catalysts shows certain regularities. The main increase of the conversion of limonene was observed for the OR catalyst—catalyst obtained without any activating agent. Catalysts obtained in the presence of activators were slightly less active, because the conversion obtained over them was 10% lower than for the OR catalyst. A comparison of the selectivities of the products shows that for all studied catalysts, the main reaction product was perillyl alcohol (allylic oxidation at position seven). The second preferred direction of oxidation was epoxidation at the 1,2-position and formation of 1,2-epoxylimonene, followed by hydration of the epoxide to diol. Moreover, for the ORNaOH catalyst obtained with NaOH as the activator, a considerable increase was observed in the selectivity of 1,2-epoxylimonene, and this epoxide was stable under the reaction conditions and did not undergo hydration to diol. For this catalyst, there was a decrease in the selectivities of carveol and carvone (products of oxidation at position six). For the catalyst obtained in the presence of KOH as the activator, there was an increase of 10% in the selectivity of perillyl alcohol, and a decrease in the selectivity of 1,2-epoxylimonene. Moreover, this epoxide compound was unstable under the reaction conditions and was easily transformed to diol, which caused

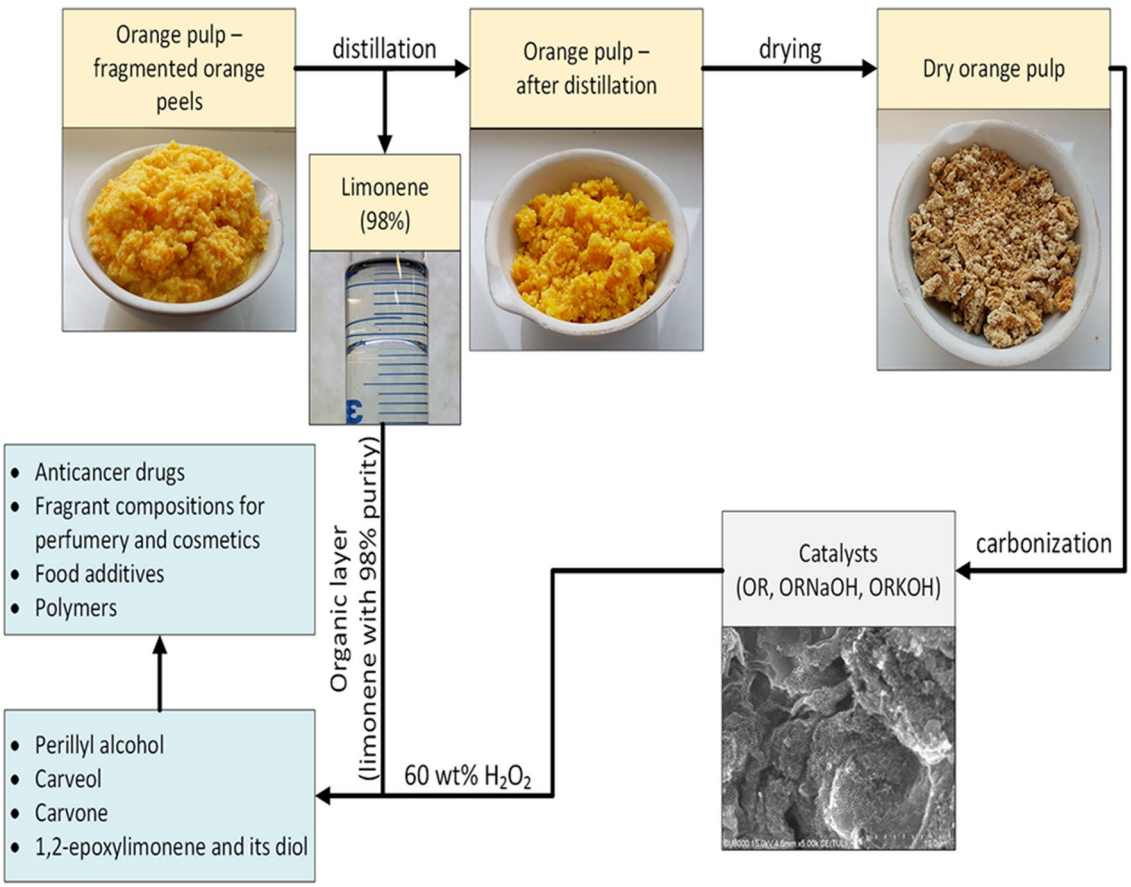

Fig. 7 Method of utilization of waste orange pulp as the source of natural limonene and, after its extraction, as catalyst for the oxidation of limonene to important oxygenated compounds

the increase in the selectivity of 1,2-epoxylimonene diol. The selectivities of carveol and carvone were comparable with the selectivities of these compounds over the ORNaOH catalyst. This change in selectivity can be explained in terms of basic sites of the carbonaceous materials treated with NaOH and KOH.

The results show that it is possible to use waste orange pulp as both the source of limonene and, after separation of this compound and carbonization, as catalysts for the oxidation of limonene to valuable oxygenated derivatives. Analyses of these catalysts showed that the activity and the selectivity of a catalyst depend on the method of preparation. By changing the method of preparation, it is possible to obtain a catalyst that is more selective in the direction of perillyl alcohol. For the production of 1,2-epoxylimonene, the catalyst that was modified with NaOH should be used. Figure 7 presents the workflow scheme that was presented in this work.

4 Conclusions

The research presented an ecological processing method that utilizes orange pulp prepared from waste orange peels, a renewable resource obtained from the orange juice industry. This pulp is not only the source of natural limonene, but also the source of active carbonaceous catalysts for the oxidation of limonene to perillyl alcohol (main product), 1,2-epoxylimonene and its diol, and, in lesser amounts, to carveol and carvone. The use of KOH as an activating agent led to an increase in the selectivities of perillyl alcohol and 1,2-epoxylimonene diol at all the temperatures that were studied, whereas the use of NaOH increased the selectivities of these two products at 80 °C and 140 °C. The oxidation is performed at very mild conditions by the use of an environmentally friendly oxidant—hydrogen peroxide.

Acknowledgements JL is a Serra Hunter Fellow and is grateful to ICREA Academia program and GC 2017 SGR 128.

Compliance with ethical standards

Conflict of interest The authors declare that they have no conflict of interest.

References

1. Rezzadori K, Benedetti S, Amante ER (2012) Proposals for the residues recovery: orange waste as raw material for new products. Food Bioprod Process 90:606–614. https://doi.org/10.1016/j.fbp.2012.06.002
2. Kimball DA (1999) Citrus processing, A Chapman & Hall food science book. Aspen Publishers, Maryland
3. Braddock RJ (1995) By-products of citrus fruit. Food Technol 49:74–77
4. Sahraoui N, Abert Vian M, El Maataoui M, Boutekedjiret C, Chemat F (2011) Valorization of citrus by-products using microwave steam distillation (MSD). Innov Food Sci Emerg Technol 12:163–170. https://doi.org/10.1016/j.ifset.2011.02.002
5. Hendrix CM, Redd JB (1999) Chemistry and technology of citrus juices and by-products. In: Ashurst PR (ed) Production and packaging of non-carbonated fruit juices and fruit beverages, 2nd edn. Springer Science + Business Media, New York, pp 53–87
6. Lis-Balchin M, Ochoka RJ, Deans SG, Asztemborska M, Haret S (1996) Bioactivity of the enantiomers of limonene. Med Sci Res 24:309–310
7. Gupta A, Stratton SP, Myrdal PB (2005) An HPLC method for quantitation of perillyl alcohol in a topical pharmaceutical cream formulation. J Pharm Biomed Anal 37:447–452. https://doi.org/10.1016/j.jpba.2004.02.039
8. Stark MJ, Burke DY, McKinzie JH, Ayoubi AS, Crowell PL (1995) Chemotherapy of pancreatic cancer with the monoterpene perillyl alcohol. Cancer Lett 96:15–21. https://doi.org/10.1016/0304-3835(95)03912-G
9. Suhail MM, Yang Q, Cao QA, Fung KM, Postier RG, Woolley C, Young G, Zhang J, Lin HK (2012) Frankincense essential oil prepared from hydrodistillation of Boswellia sacra gum resins induces human pancreatic cancer cell death in cultures and in a xenograft murine model. Compl Alter Med 12:253. https://doi.org/10.1186/1472-6882-12-253
10. Jaafari A, Tilaoui M, Mouse HA, M'bark LA, Aboufatima R, Chait A, Lepoivre M, Zyad A (2012) Comparative study of the antitumor effect of natural monoterpenes: relationship to cell cycle analysis. Braz J Pharm. https://doi.org/10.1590/S0102-695X2012005000021
11. Kapica J, Pełech R, Przepiórski J, Morawski AW (2002) Kinetics of the adsorption of copper and lead ions from aqueous solution on to WD-ekstra activated carbon. Adsorpt Sci Technol 20:441–452. https://doi.org/10.1260/026361702320644734
12. Serafin J, Narkiewicz U, Morawski AW, Wróbel RJ, Michalkiewicz B (2017) Highly microporous activated carbons from biomass for CO_2 capture and effective micropores at different conditions. J Utilz CO2 18:73–79. https://doi.org/10.1016/j.jcou.2017.01.006
13. Kapica-Kozar J, Piróg E, Kusiak-Nejman E, Wróbel RJ, Gęsikiewicz-Puchalska A, Morawski AW, Narkiewicz U, Michalkiewicz B (2017) Titanium dioxide modified with various amines used as sorbents of carbon dioxide. New J Chem 41:1549–1557. https://doi.org/10.1039/C6NJ02808J
14. Athappan A, Sattler ML, Sethupathi S (2015) Selective catalytic reduction of nitric oxide over cerium-doped activated carbons. J Environ Chem Eng 3:2502–2513. https://doi.org/10.1016/j.jece.2015.08.028
15. Meryemoglu B, Irmak S, Hasanoglu A (2016) Production of activated carbon materials from kenaf biomass to be used as catalyst support in aqueous-phase reforming process. Fuel Process Technol 151:59–63. https://doi.org/10.1016/j.fuproc.2016.05.040
16. Zhang C, Wang T, Liu X, Ding Y (2016) Selective oxidation of glycerol to lactic acid over activated carbon supported Pt catalyst

in alkaline solution. Chinese J Catal 37:502–509. https://doi.org/10.1016/S1872-2067(15)61055-5
17. Shi W, Gao H, Yu J, Jia M, Dai T, Zhao Y, Xu J, Li G (2016) One-step synthesis of N-doped activated carbon with controllable Ni nanorods for ethanol oxidation. Electrochim Acta 220:486–492. https://doi.org/10.1016/j.electacta.2016.10.051
18. Simaioforidou A, Papastergiou M, Margellou A, Petrakis D, Louloudi M (2017) Activated vs. pyrolytic carbon as support matrix for chemical functionalization: efficient heterogeneous non-heme Mn(II) catalysts for alkene oxidation with H_2O_2. J Mol Catal A Chem 426:516–525. https://doi.org/10.1016/j.molcata.2016.08.033
19. Zong MH, Duan ZQ, Lou WY, Smith TJ, Wu H (2007) Preparation of a sugar catalyst and its use for highly efficient production of biodiesel. Green Chem 9:434–437. https://doi.org/10.1039/B615447F
20. Mar WW, Somsook E (2012) Sulfonic-functionalized carbon catalyst for esterification of high free fatty acid. Procedia Eng 32:212–218. https://doi.org/10.1016/j.proeng.2012.01.1259
21. Młodzik J, Wróblewska A, Makuch E, Wróbel RJ, Michalkiewicz B (2016) Fe/EuroPh catalysts for limonene oxidation to 1,2-epoxylimonene, its diol, carveol, carvone and perillyl alcohol. Catal Today 268:111–120. https://doi.org/10.1016/j.cattod.2015.11.010
22. Wróblewska A, Makuch E, Młodzik J, Michalkiewicz B (2017) Fe-carbon nanoreactors obtained from molasses as efficient catalysts for limonene oxidation. Green Process Synth 6:397–401. https://doi.org/10.1515/gps-2016-0148
23. Michalkiewicz B, Wróblewska A, Gawarecka A, Miądlicki P, Serafin J (2016) Pol Patent 416376
24. Fang X, Chen C, Liu Z, Liu P, Zheng N (2011) A cationic surfactant assisted selective etching strategy to hollow mesoporous silica spheres. Nanoscale 3:1632–1639. https://doi.org/10.1039/C0NR00893A
25. Ganguly S, Zhou C, Morelli D, Sakamoto J, Uher C, Brock SL (2011) Synthesis and evaluation of lead telluride/bismuth antimony telluride nanocomposites for thermoelectric applications. J Solid State Chem 184:3195–3201. https://doi.org/10.1016/j.jssc.2011.09.031
26. Jacobs G, Ghadiali F, Pisanu A, Borgna A, Alvarez WE, Resasco DE (1999) Characterization of the morphology of Pt clusters incorporated in a KL zeolite by vapor phase and incipient wetness impregnation. Influence of Pt particle morphology on aromatization activity and deactivation. Appl Catal A 188:79–98. https://doi.org/10.1016/S0926-860X(99)00235-5
27. Lee EL, Wachs IE (2008) Molecular design and in situ spectroscopic investigation of multilayered supported $M_1Ox/M_2Ox/SiO_2$ catalysts. J Phys Chem C 112:20418–20428. https://doi.org/10.1021/jp805265m
28. Gregg SJ, Sing KSW (1982) Adsorption, surface area, and porosity, 2nd edn. Academic Press, London
29. Wenelska K, Michalkiewicz B, Chen X, Mijowska E (2014) Pd nanoparticles with tunable diameter deposited on carbon nanotubes with enhanced hydrogen storage capacity. Energy 75:549–554. https://doi.org/10.1016/j.energy.2014.08.016
30. Gelb LD, Gubbins KE, Radhakrishnan R, Sliwinska-Bartowiak M (1999) Phase separation in confined systems. Rep Prog Phys 62:1573–1659. https://doi.org/10.1088/0034-4885/62/12/201
31. Ravikovitch P, Vishnyakov A, Russo R, Neimark AV (2000) Unified approach to pore size characterization of microporous carbonaceous materials from N_2, Ar, and CO_2 adsorption isotherms. Langmuir 16:2311–2320. https://doi.org/10.1021/la991011c
32. Sreńscek-Nazzal J, Kamińska W, Michalkiewicz B, Koren ZC (2013) Production, characterization and methane storage potential of KOH-activated carbon from sugarcane molasses. Ind Crop Prod 47:153–159. https://doi.org/10.1016/j.indcrop.2013.03.004
33. Gong J, Michalkiewicz B, Chen X, Mijowska E, Liu J, Jiang Z, Wen X, Tang T (2014) Sustainable conversion of mixed plastics into porous carbon nanosheets with high performances in uptake of carbon dioxide and storage of hydrogen. ACS Sustain Chem Eng 2:2837–2844. https://doi.org/10.1021/sc500603h
34. Sreńscek-Nazzal J, Narkiewicz U, Morawski A, Wróbel R, Gęsikiewicz-Puchalska A, Michalkiewicz B (2016) Modification of commercial activated carbons for CO_2 adsorption. Acta Phys Pol A 129:394–401. https://doi.org/10.12693/APhysPolA.129.394
35. Malengreaux CM, Pirard SL, Leonard G, Mahy JG, Herlitschke M, Klobes B, Hermann R, Heinrichs B, Bartlett JR (2017) Study of the photocatalytic activity of Fe^{3+}, Cr^{3+}, La^{3+} and Eu^{3+} single-doped and co-doped TiO_2 catalysts produced by aqueous sol-gel processing. J Alloy Compd 691:726–738. https://doi.org/10.1016/j.jallcom.2016.08.211
36. Marszewska J, Jaroniec M (2017) Tailoring porosity in carbon spheres for fast carbon dioxide adsorption. J Colloid Interf Sci 487:162–174. https://doi.org/10.1016/j.jcis.2016.10.033
37. Gun'ko VM, Leboda R, Skubiszewska-Zięba J, Charmas B, Oleszczuk P (2005) Carbon adsorbents from waste ion-exchange resins. Carbon 43:1143–1150. https://doi.org/10.1016/j.carbon.2004.09.032
38. Wróblewska A (2014) The epoxidation of limonene over the TS-1 and Ti-SBA-15 catalysts. Molecules 19:19907–19922. https://doi.org/10.3390/molecules191219907
39. Wróblewska A, Makuch E, Miądlicki P (2016) The studies on the limonene oxidation over the microporous TS-1 catalyst. Catal Today 268:121–129. https://doi.org/10.1016/j.cattod.2015.11.008